

# Effects of charge spreading on resolution of optically addressed spatial light modulators

Li Wang and Garret Model

Department of Electrical and Computer Engineering and Center for Optoelectronic Computing Systems,  
University of Colorado, Boulder, Colorado 80309-0425

Received July 11, 1994

A transient charge-transport model is developed to evaluate the resolution limits of optically addressed spatial light modulators. The effect of bulk charge diffusion on resolution is largely independent of the mobility in the semiconductor layer, and the resolution is limited by the lateral diffusion length of charge carriers in transit. The effects of charge drift, diffusion, and trapping at the interface between the semiconductor and the light-modulating layer depend strongly on the interface properties. The resolution ranges from 2 to 700 line pairs/mm for respective diffusion lengths of 16.1 to 0.16  $\mu\text{m}$  at the interface.

Spatial resolution is one of the crucial performance parameters in optically addressed spatial light modulators (OASLM's). It is determined by several transfer processes in these devices, which include the transfer characteristic of input image intensity to charge distribution in the photosensitive layer, to the voltage distribution in the light-modulating layer, and finally to the phase or amplitude modulation of the output image. Photogenerated charge carriers in the photosensitive layer are separated by the applied electric field and accumulate at the semiconductor-liquid-crystal (LC) interface in LC OASLM's<sup>1-3</sup> or at the semiconductor-dielectric interface in multiple-quantum well (MQW) devices<sup>4</sup> and Pockels readout modulators (PROM's).<sup>5,6</sup> During the transfer process from input image intensity to charge distribution, charge spreading is inevitable and deteriorates the resolution of OASLM's. Various charge-spreading mechanisms are illustrated in Fig. 1. By taking into account charge drift in the bulk semiconductor layer (process a in Fig. 1), a charge-transport model has successfully simulated the modulation transfer function (MTF) in PROM's.<sup>7</sup> Another charge-transport model has been developed that analyzes the charge drift and diffusion effects in a bulk semiconductor layer (processes a and b in Fig. 1) for steady-state operation of MQW devices.<sup>8</sup> By neglecting the charge-spreading effects, one can evaluate the resolution of OASLM's with the electrostatic models for the transfer process from charge distribution to voltage distribution.<sup>9,10</sup>

It is crucial to model the transient charge transport because the charge distribution in the photosensitive layer varies with time, as does the voltage in the light-modulating layer. Even when a steady-state image is written onto the device, the charge transport is transient because both LC OASLM's and MQW devices are operated under an ac electric field with 1–50-kHz frequencies. In this Letter the simulation results from a comprehensive transient charge-transport model are presented. This model includes both the diffusion effect in the bulk semiconductor and the drift and diffusion effects at the interface (processes b and c in Fig. 1). The

MTF, which is suitable for the linear bulk diffusion effect, and an effective MTF, which is defined in this Letter for the nonlinear charge-spreading effects at the interface, are used to characterize the resolution limits of OASLM's associated with the transfer process from input image intensity to charge distribution. Once the charge distribution at the interface is calculated from this model and the previous charge-transport model that considers bulk drift (process a),<sup>7</sup> one can use the electrostatic models<sup>9,10</sup> to obtain the voltage distribution in the light-modulating layer, and the resolution limits of OASLM's can be accurately predicted.

Charge diffusion in a bulk semiconductor may be described by the following rate equation.<sup>11</sup> The sheet concentration of photogenerated charge carriers in transit,  $N_{\text{trans}}(x, t)$ , in units of inverse centimeters squared, is given by

$$\frac{\partial N_{\text{trans}}(x, t)}{\partial t} = D_{\parallel} \frac{\partial^2 N_{\text{trans}}(x, t)}{\partial x^2} + g(x, t) - \frac{N_{\text{trans}}(x, t)}{\tau_r} - \frac{N_{\text{trans}}(x, t)}{T}, \quad (1)$$

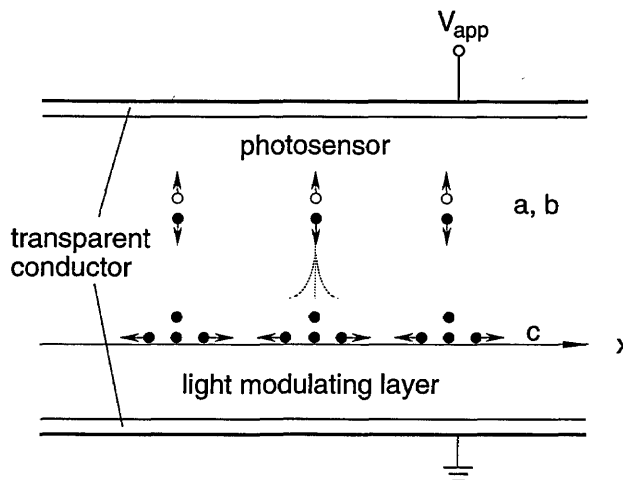


Fig. 1. Charge-spreading mechanisms in an OASLM: a, drift and b, diffusion in the bulk photosensor layer; c, drift and diffusion at the interface.

where  $D_{\parallel}$  is the lateral diffusion coefficient of charge carriers in the semiconductor bulk,  $g(x, t)$  is the charge-carrier generation rate (in units of  $\text{cm}^{-2} \text{s}^{-1}$ ) and is assumed to be proportional to the input image intensity,  $\tau_r$  is the recombination lifetime, and  $T$  is the average transit time for charge carriers from the bulk semiconductor to the interface and is a constant to a first-order approximation. The last term in Eq. (1) can be considered the charge-collection rate at the interface  $g_{\text{col}}(x, t)$ .

We can find an analytical solution to Eq. (1) by assuming that  $g(x, t) = g_0[1 + m \cos(2\pi f x)]$  after  $t = 0$ , where  $g_0$  is the spatial average charge-generation rate,  $m$  is the modulation, and  $f$  is the spatial frequency in units of line pairs per millimeter (lp/mm). Usually the transit time or the recombination lifetime is much shorter than the write time  $t$ , in which case the analytical solution is simplified to

$$N_{\text{trans}}(x, t) = g_0 \tau_0 \left[ 1 + \frac{m}{1 + 4\pi^2 D_{\parallel} \tau_0 f^2} \cos(2\pi f x) \right], \quad t \gg T \text{ or } \tau_r, \quad (2)$$

where  $\tau_0$  is the effective lifetime and is equal to  $\tau_r T / (\tau_r + T)$ . The charge-collection rate at the interface can be found by substitution of Eq. (2) into the last term in Eq. (1). The MTF that is due to this bulk diffusion effect, which is defined as the ratio of the charge-collection rate modulation to the charge-generation rate modulation, is  $\text{MTF} = 1/(1 + 4\pi^2 D_{\parallel} \tau_0 f^2)$ . The critical spatial frequency at which the MTF decreases to 50% is  $f_c = 1/(2\pi \sqrt{D_{\parallel} \tau_0})$ , where  $\sqrt{D_{\parallel} \tau_0}$  is the characteristic length over which carriers diffuse laterally during their transit.

Figure 2 shows the critical spatial frequencies for various values of lateral mobility and effective lifetime. The mobility is converted from the diffusion coefficient  $D_{\parallel}$  through the Einstein relationship. Mobilities of charge carriers (usually electrons) in hydrogenated amorphous silicon ( $\alpha$ -Si:H) are very small ( $\sim 0.1$ – $1 \text{ cm}^2/\text{V s}$ ), but the relatively long transit time that is due to the small vertical mobility, and the long recombination lifetime for electrons, result in a small but nonnegligible diffusion length  $\sqrt{D_{\parallel} \tau_0}$ . Photosensors of  $\alpha$ -Si:H that are used in OASLM's are located at the upper-left corner of Fig. 2 and give relatively high resolution ( $>100 \text{ lp/mm}$ ). On the other hand, photosensors of crystalline semiconductors such as GaAs, AlGaAs, and Si that are used in MQW devices and other OASLM's have very high lateral mobilities ( $\sim 100$ – $3000 \text{ cm}^2/\text{V s}$ ). One might expect that the large bulk diffusion would reduce the resolution in these devices. However, the very short transit time, which is due to the large vertical mobility, results instead in a relatively small diffusion length  $\sqrt{D_{\parallel} \tau_0}$ . Such crystalline semiconductor photosensors are located at the lower-right corner of Fig. 2 and also give high resolution in OASLM's ( $>100 \text{ lp/mm}$ ). Thus the resolution is largely independent of the mobility in the bulk of the semiconductor photosensor.

Once the charge carriers arrive at the photosensor-light-modulating layer interface, they diffuse and drift laterally until they are trapped or the write period ends. This charge-spreading effect

further reduces the modulation in the charge distribution. It is assumed in the analysis that the charge carriers deposited at the interface are released and/or recombined with the opposite-sign charge carriers during the following reset or erase period. Rate equations describing drift, diffusion, and trapping at the interface are<sup>11</sup>

$$\frac{\partial N_{\text{free}}(x, t)}{\partial t} = \mp \frac{1}{q} \frac{\partial J_{\text{free}}(x, t)}{\partial x} + g_{\text{col}}(x, t) - \frac{N_{\text{free}}(x, t)}{\tau_t}, \quad (3a)$$

$$\frac{\partial N_{\text{trap}}(x, t)}{\partial t} = \frac{N_{\text{free}}(x, t)}{\tau_t}, \quad (3b)$$

where  $N_{\text{free}}(x, t)$  and  $N_{\text{trap}}(x, t)$  are the free and trapped charge concentrations accumulated at the interface, respectively,  $g_{\text{col}}(x, t)$  is the charge-collection rate, and  $\tau_t$  is the trapping time, which depends strongly on the interface properties. The minus in front of the first term on the right-hand side of Eq. (3a) is for holes, and the plus is for electrons.  $J_{\text{free}}(x, t)$  in Eq. (3a) is the sheet current density resulting from diffusion and drift of the free charge carriers at the interface and is written as<sup>11</sup>

$$J_{\text{free}}(x, t) = q \mu_s E_x(x, t) N_{\text{free}}(x, t) \mp q D_s \frac{\partial N_{\text{free}}(x, t)}{\partial x}, \quad (4)$$

where  $D_s$  and  $\mu_s$  are the diffusion coefficient and the mobility of charge carriers at the interface and may be different from those in the bulk region.  $E_x(x, t)$  is the lateral ( $x$ -component) electric field at the interface and is calculated from  $N_{\text{free}}(x, t)$  and  $N_{\text{trap}}(x, t)$  by solution of the Poisson equations. The minus in front of the last term on the right-hand side of Eq. (4) is for holes, and the plus is for electrons.

Equations (3a) and (3b) are nonlinear partial differential equations, and we have solved them numerically, using the Crank–Nicolson implicit

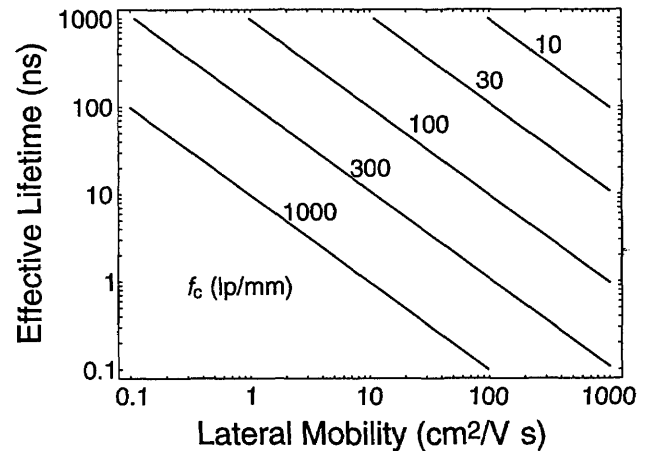


Fig. 2. Effect of bulk diffusion: plot of the critical spatial frequency (at which the effective MTF falls to 50%) versus lateral mobility and the effective lifetime in the semiconductor.

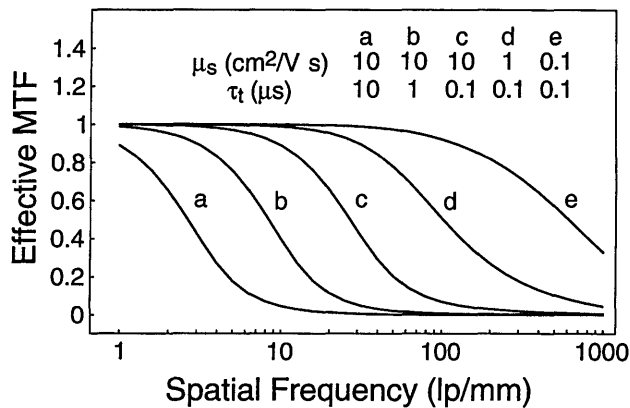


Fig. 3. Effective MTF that is due to the charge-spreading effects at the interface. The mobility and the trapping time are shown for each curve. The spatial average in the charge-collection rate is assumed to be  $5 \times 10^{13} \text{ cm}^{-2} \text{ s}^{-1}$ , and its modulation is unity. The thicknesses of the photosensor and the LC layers are 3 and 1  $\mu\text{m}$ , respectively. The dielectric constants for the photosensor and the LC are  $12\epsilon_0$  (e.g., for  $\alpha\text{-Si:H}$ ) and  $4\epsilon_0$ , respectively, where  $\epsilon_0$  is the permittivity of free space.

finite-difference method.<sup>12</sup> The total charge distribution at the interface is the summation of the free charge  $N_{\text{free}}(x, t)$  and the trapped charge  $N_{\text{trap}}(x, t)$ . The spatial average and the first Fourier harmonic component of the total charge distribution are calculated numerically first. Then the effective modulation in the total charge distribution is evaluated as the ratio of the first Fourier harmonic to the spatial average. The effective MTF for this charge-spreading process is defined as the ratio of the effective modulation in the total charge distribution to the modulation in the charge-collection rate at the interface. This definition of an effective MTF is consistent with the small-amplitude approximation in which higher-order Fourier harmonics are usually neglected. Figure 3 shows the calculated effective MTF at the end of the write period ( $t = 0.5 \text{ ms}$ ) with spatial frequency for various combinations of mobility and trapping time in a LC OASLM with an  $\alpha\text{-Si:H}$  photosensor. Charge carriers with lower mobility or shorter trapping time at the interface have less chance or time to drift and diffuse before they are trapped by the interface states, and thus they result in higher resolutions. We also have found in the numerical solution that the same  $\sqrt{D_s \tau_t}$  values (distance over which carriers diffuse before they are trapped at the interface) give similar effective MTF curves. It is clear from Fig. 3 that decreasing the mobility or the trapping time at the interface can significantly improve the resolution of OASLM's.

Creation of trapping or defect states at the interface may reduce the mobility and the trapping time and thus improve the resolution. This has been done intentionally in MQW devices with a low-temperature-grown interfacial layer between the MQW region and the dielectric layer.<sup>4</sup> Alternatively, one can preserve the resolution of OASLM's with crystalline semiconductors by pixelating the in-

terface to impede the charge-spreading effect.<sup>1,3</sup> In some LC OASLM's that have  $\alpha\text{-Si:H}$  photosensors,<sup>13</sup> the measured MTF curves fit the electrostatic model<sup>9</sup> very well. This indicates that the resolutions in these devices are limited by the transfer process from charge distribution to voltage distribution. In other LC OASLM's with similar structures<sup>2,14</sup> the measured resolutions are much lower than the predictions from the electrostatic model and appear to be limited by charge-spreading effects at the interface.

In conclusion, we have developed a transient model to evaluate the effects of charge spreading on resolution of OASLM's. Diffusion in the bulk is largely independent of the mobility in the semiconductor and is negligible in most cases. The effects of charge drift and diffusion at the interface depend strongly on the interface properties. Decreasing the mobility or the trapping time can improve the resolution. The spatial resolution is reduced further when the total charge distribution is converted to voltage distribution in the light-modulating layer. The transient charge-transport model should be used together with the electro-static models<sup>9,10</sup> and a bulk drift model<sup>7</sup> for accurate calculation of the resolution limits of OASLM's.

We acknowledge support from National Science Foundation Engineering Research Center grant ECD9015128 and by the Colorado Advanced Technology Institute, an agency of the State of Colorado.

## References

1. U. Efron, J. Grinberg, P. O. Braatz, M. J. Little, P. G. Reif, and R. N. Schwartz, *J. Appl. Phys.* **57**, 1356 (1985).
2. G. Moddel, K. M. Johnson, W. Li, R. A. Rice, L. A. Pagano-Stauffer, and M. A. Handschy, *Appl. Phys. Lett.* **55**, 537 (1989).
3. D. Armitage, J. I. Thackara, and W. D. Eades, *Appl. Opt.* **28**, 4763 (1989).
4. A. Partovi, A. M. Glass, D. H. Olson, G. J. Zydzik, and H. M. O'Bryan, *Appl. Phys. Lett.* **62**, 464 (1993).
5. B. A. Horwitz and F. J. Corbett, *Opt. Eng.* **17**, 353 (1978).
6. Y. Nagao, H. Sakata, and Y. Mimura, *Appl. Opt.* **31**, 3966 (1992).
7. J. Chen and T. Minemoto, *J. Opt. Soc. Am. A* **6**, 1281 (1989).
8. D. D. Nolte, *Opt. Commun.* **92**, 199 (1992).
9. W. R. Roach, *IEEE Trans. Electron. Dev.* **ED-21**, 453 (1974).
10. Y. Owechko and A. R. Tanguay, Jr., *J. Opt. Soc. Am. A* **1**, 635 (1984).
11. R. S. Muller and T. I. Kamins, *Device Electronics for Integrated Circuits*, 2nd ed. (Wiley, New York, 1986), Chaps. 1 and 5.
12. W. F. Ames, *Numerical Methods for Partial Differential Equations*, 2nd ed. (Academic, New York, 1977).
13. S. Fukushima, T. Kurokawa, and M. Ohno, *Appl. Opt.* **31**, 6859 (1992).
14. D. Williams, S. G. Latham, C. M. J. Powles, M. A. Powell, R. C. Chittick, A. P. Sparks, and N. Collings, *J. Phys. D* **21**, S156 (1988).